Sensor data fusion for determine object position

Emil Iontchev[1], Rosen Miletiev[2], Petar Kapanakov[3] and Lachezar Hristov[4]

Abstract: **The paper represents the algorithm which combines the sensor data to determine the object position in the space by Extended Kalman Filter (EKF). Two different filters are proposed – nonlinear Kalman filter and linear one with quaternions. Also the algorithm for rejection of the external magnetic disturbances is chosen to correct the magnetometer data. Another low-pass filter is applied to the accelerometer data. The proposed algorithms are tested on stationary and on moving platforms to calculate the rotation angles of the kid car seat.**

Keywords – **accelerometer, gyroscope, magnetometer, Kalman filter**

I. INTRODUCTION

Object position determination is the major task of the human life and it is solved by different methods. Nowadays, the outdoor position may be obtained easily by using the global navigation positioning systems (GNSS) [1]. The indoor navigation task also may be solved using inertial navigation systems (INS), beacons, etc. [2], but sometimes there is a necessity to combine the navigation systems to overcome some specific disadvantages, such as the integration error in the INS systems, which decision is proposed by Rudolf Kalman, [3] known as Kalman filter. This filter is also used to combine the sensor data from different measurement systems. The alternative of Kalman filter is the complementary filter [4,5] which may be implemented easily in the embedded system due to its low complexity. It uses the constant values for the low and high pass filters, while the Kalman filter calculates the sensor noise and dynamically changes these values. The Kalman Filter is, however, known to provide an optimal estimate of the unknown state for a linear dynamic system with Gaussian distribution.

The current paper discusses the Kalman filter algorithm which is used to calculate the rotation angles of the kid car seat. The algorithm verification is shown in the stationary and moving situations and the results are commented. By integrating data from accelerometers and gyroscope, mounted on the car seat, we were able to predict and calculate its position.

[1] Emil Iontchev is with the Higher School of Transport "T. Kableshkov" 158 Geo Milev Street, Sofia 1574, Bulgaria, E-mail: e_iontchev@yahoo.com

[2] Rosen Miletiev is with the Faculty of Telecommunications at Technical University of Sofia, 8 Kl. Ohridski Blvd, Sofia 1000, Bulgaria. E-mail: miletiev@tu-sofia.bg

[3] Petar Kapanakov is with the Faculty of Telecommunications at Technical University of Sofia, 8 Kl. Ohridski Blvd, Sofia 1000, Bulgaria. E-mail: peshoteslata2@abv.bg

[4] Lachezar Hristov is with the Higher School of Transport "T. Kableshkov" 158 Geo Milev Street, Sofia 1574, Bulgaria, E-mail: Lachezar.Hristov@outlook.com

II. ALGORITHM DESCRIPTION OF THE DATA COMBINATION

The rotation angles calculation of the object (kid car seat) is accomplished by 9DoF inertial measurement system, which is capable of reading the linear accelerations and angular velocities and magnetometer data too. The data of these nine degrees of freedom are combined to calculate the three Euler angles in the inertial coordinate system. The transformation of the coordinate system to the inertial one is based on the rotation matrix Rxyz [6].

The combination of the sensor data is made using the Kalman algorithm, which is well known and is implemented in many systems [7,8]. The object mathematical model assumes that the actual measurement at any time is related to the current state and the system model may be written as [9]:

(1) $\mathbf{x_{k+1} = Ax_k + w_k}$

(2) $\mathbf{z_k = Hx_k + v_k}$

where, $\mathbf{x_k}$ – denotes the column vector (nx1) of state estimate, $\mathbf{z_k}$ - column vector (mx1) of measurements, A - state transition matrix (mxn) which is applied to the previous state, H – the observation matrix (mxn) which maps the true state space into the observed space $\mathbf{w_k}$ – model noise and $\mathbf{v_k}$ – measurement noise, which are normally distributed and are independent. In the filter algorithms the noise is represented by the matrices Q(covariance matrix of $\mathbf{w_k}$) and R(covariance matrix of $\mathbf{v_k}$), which is used to calculated the Kalman coefficient

(3) $\mathbf{K_k = \frac{P_k^- H^T}{HP_k^- H^T + R}}$.

The practical implementation of the Kalman Filter is often difficult due to the difficulty of getting a good estimate of the noise covariance matrices. Several methods for the noise covariance estimation have been proposed such as autocovariance least-squares (ALS) technique. The predicted (*a priori*) state estimate is calculated by (4):

(4) $\mathbf{\hat{x}_k = (1 - K_k)\hat{x}_k^- + K_k z_k}$

In the same time the Q matrix is used to obtain the predicted (*a priori*) error covariance $\mathbf{P_{k+1}^-}$:

(5) $\mathbf{P_{k+1}^- = AP_k^- A^T + Q}$

It is better to choose the smaller Q values and bigger R values if we want to decrease the state variations.

The system model for calculation of the Euler angles with quaternions (q) is given by the equation (6):

(6) $\begin{Bmatrix} \mathbf{q_1} \\ \mathbf{q_2} \\ \mathbf{q_3} \\ \mathbf{q_4} \end{Bmatrix}_{k+1} = \left(\mathbf{I} + \Delta t \frac{1}{2} \begin{bmatrix} \mathbf{0} & -\mathbf{p} & -\mathbf{q} & -\mathbf{r} \\ \mathbf{p} & \mathbf{0} & \mathbf{r} & -\mathbf{q} \\ \mathbf{q} & -\mathbf{r} & \mathbf{0} & \mathbf{p} \\ \mathbf{r} & \mathbf{q} & -\mathbf{p} & \mathbf{0} \end{bmatrix} \begin{Bmatrix} \mathbf{q_1} \\ \mathbf{q_2} \\ \mathbf{q_3} \\ \mathbf{q_4} \end{Bmatrix}_k \right)$

where **p, q, r** denote the angular velocities from the gyroscope measurements.

The transition matrix is given by (7):

$$(7) A = I + \Delta t \frac{1}{2} \begin{bmatrix} 0 & -p & -q & -r \\ p & 0 & r & -q \\ q & -r & 0 & p \\ r & q & -p & 0 \end{bmatrix}.$$

The quaternion values are calculated from the Euler angles according to the equation (8):

$$(8) \begin{pmatrix} q_1 \\ q_2 \\ q_3 \\ q_4 \end{pmatrix} = \begin{cases} \cos\frac{\phi}{2}\cos\frac{\theta}{2}\cos\frac{\psi}{2} + \sin\frac{\phi}{2}\sin\frac{\theta}{2}\sin\frac{\psi}{2} \\ \sin\frac{\phi}{2}\cos\frac{\theta}{2}\cos\frac{\psi}{2} - \cos\frac{\phi}{2}\sin\frac{\theta}{2}\sin\frac{\psi}{2} \\ \cos\frac{\phi}{2}\sin\frac{\theta}{2}\cos\frac{\psi}{2} + \sin\frac{\phi}{2}\cos\frac{\theta}{2}\sin\frac{\psi}{2} \\ \cos\frac{\phi}{2}\cos\frac{\theta}{2}\sin\frac{\psi}{2} - \sin\frac{\phi}{2}\sin\frac{\theta}{2}\cos\frac{\psi}{2} \end{cases}$$

If the Euler angles are used as state estimates the nonlinear model is used according to the equation (9) and (10):

$$(9) \begin{pmatrix} \dot{\phi} \\ \dot{\theta} \\ \dot{\psi} \end{pmatrix} = \begin{bmatrix} p + q\sin\phi\tan\theta + r\cos\phi\tan\theta \\ q\cos\phi - r\sin\phi \\ q\sin\phi\sec\theta + r\cos\phi\sec\theta \end{bmatrix} + w_k \equiv f(x) + w$$

$$(10) z = \begin{bmatrix} 1 & 0 & 0 \\ 0 & 1 & 0 \end{bmatrix} \begin{Bmatrix} \phi \\ \theta \\ \psi \end{Bmatrix} + v_k \equiv hf(x) + v$$

The difference between the above model and the linear model(1,2) is that the linear matrix equation has been changed into nonlinear form as following Ax_k to f (x) and Hx_k to hf (x). To implement an extended Kalman filter the Jacobian of equation (9) must be known. This is defined as following (11):

$$(11) A = \begin{bmatrix} \frac{\partial f_1}{\partial \phi} & \frac{\partial f_1}{\partial \theta} & \frac{\partial f_1}{\partial \psi} \\ \frac{\partial f_2}{\partial \phi} & \frac{\partial f_2}{\partial \theta} & \frac{\partial f_2}{\partial \psi} \\ \frac{\partial f_3}{\partial \phi} & \frac{\partial f_3}{\partial \theta} & \frac{\partial f_3}{\partial \psi} \end{bmatrix}$$

In both system models, the Euler angles, determined by the accelerometer data, becomes the measurement in Kalman filter. They are stable over time but substantially deviating from the actual values, especially when additional linear accelerations affect them (12):

$$(12) \begin{bmatrix} a_x \\ a_y \\ a_z \end{bmatrix} = \begin{bmatrix} \dot{u} \\ \dot{v} \\ \dot{w} \end{bmatrix} + \begin{bmatrix} 0 & w & -v \\ -w & 0 & u \\ v & -u & 0 \end{bmatrix} \begin{bmatrix} p \\ q \\ r \end{bmatrix} + g \begin{bmatrix} \sin\theta \\ -\cos\theta\sin\phi \\ -\cos\theta\cos\phi \end{bmatrix}$$

where u, v, w denotes the velocities and p, q, r – angular speed and a_x, a_y, a_z are accelerometer data, g – gravitational acceleration. If the system is stationary or moving with constant velocity, the equation (12) becomes as simple as following (13):

$$(13) \begin{bmatrix} f_x \\ f_y \\ f_z \end{bmatrix} = g \begin{bmatrix} \sin\theta \\ -\cos\theta\sin\phi \\ -\cos\theta\cos\phi \end{bmatrix}$$

The angles ϕ and θ are calculated according to (14) and (15)[6]:

$$(14) \theta_a = atan\left(\frac{-a_x}{\sqrt{(a_y)^2 + (a_z)^2}}\right)$$

$$(15) \phi_a = atan\left(\frac{a_y}{signa_z\sqrt{(a_z)^2 + \mu(a_x)^2}}\right)$$

The μ parameter is included in the equation to prevent the null values division. The ψ angle calculation cannot be estimated

from the accelerometer data so the magnetometer data have to be used. It is calculated according to the equation (16) [6]:

$$(16) \psi_a = atan\left(\frac{Y_h}{X_h}\right),$$

where Y_h and X_h denotes the Y and X magnetometer values respectively, which are calculated according to the magnetometer data values, corrected by the inclination angles by equation (17) and (18)[10]:

$$(17) X_h = (b_x - V_x)\cos\theta_a + (b_y - V_y)\sin\theta_a\sin\phi_a + (b_z - V_z)\sin\theta_a\cos\phi_a$$

$$(18) Y_h = (b_z - V_z)\sin\phi_a - (b_y - V_y)\cos\phi_a$$

The measured magnetometer data are distorted by the soft and hard iron effects so it is necessary to calibrate the data. The magnetometer data calibration is accomplished by the algorithm described at [11]. The six data values are used for X value calculation according to the equation (19):

$$(19) X = \begin{bmatrix} b_x[0] & b_y[0] & b_z[0] \\ b_x[1] & b_y[1] & b_z[1] \\ ... & .... & ... \\ b_x[5] & b_y[5] & b_z[5] \end{bmatrix}$$

The chosen data values are also used for parameter Y estimation according to the equation (20):

$$(20) Y = \begin{bmatrix} b_x[0]^2 + b_y[0]^2 + b_z[0]^2 \\ b_x[1]^2 + b_y[1]^2 + b_z[1]^2 \\ ... & .... & ... \\ b_x[5]^2 + b_y[5]^2 + b_z[5]^2 \end{bmatrix}$$

The results from the equations (19) and (20) are used for parameter β estimation according to the equation (21):

$$(21) \beta = (X^T X)^{-1} X^T Y$$

The calculated β values then are used for calculation of the magnetometer data disturbances (22):

$$(22) \begin{pmatrix} V_x \\ V_y \\ V_z \end{pmatrix} = \frac{1}{2}\begin{pmatrix} \beta_0 \\ \beta_1 \\ \beta_2 \end{pmatrix}$$

The obtained values are subtracted from the measured values and the calculated ones are used for the Euler angle estimation.

III. EXPERIMENTAL RESULTS

The validation of the proposed algorithm is accomplished with/via static and dynamic measurements with the MEMS inertial sensor ADIS16405 [12], produced by Analog Devices. The first test checks the static performance of the algorithm and compare the seat rotation angles with the measured ones. The test is also used to calibrate the magnetometer and compensate the soft and the hard iron effects. The calculated Euler angles before and after magnetometer calibration are shown at Figure 1 and Figure 2. The magnetometer curves in the XY coordinate systems before and after calibration are shown at Figure 3.
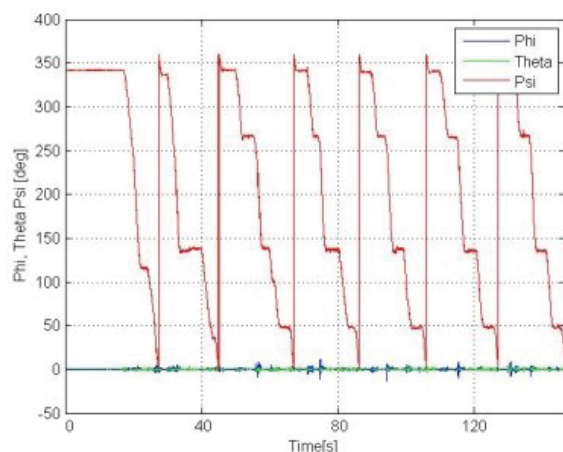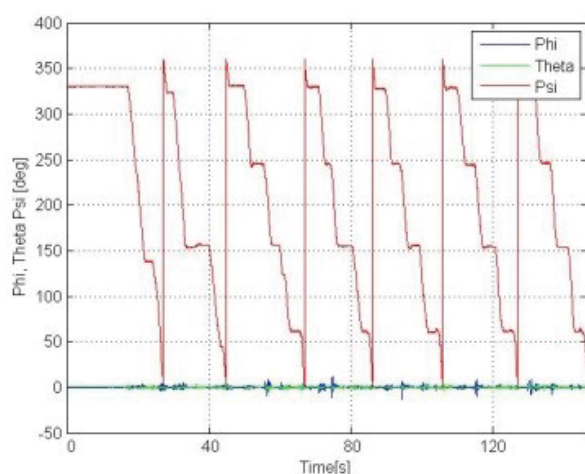
Figure 1. Euler angles before calibration

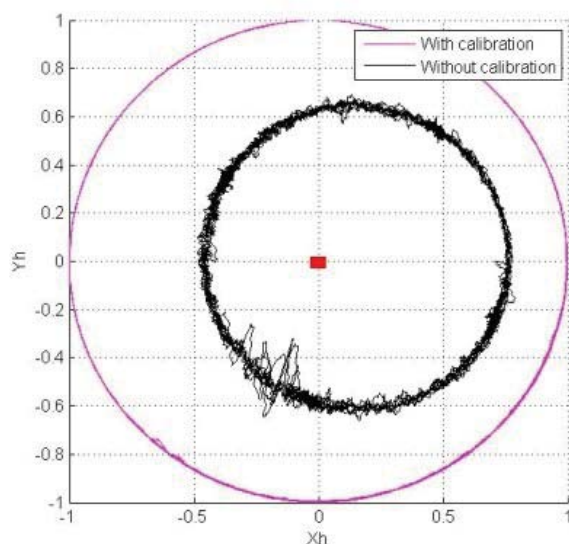Figure 2. Euler angles after calibration

Figure 3. Representation of X_h and Y_h magnetometer data before and after calibration

The dynamic test is accomplished while the inertial module is installed on the kid car seat which is specially designed for

the measurements [13,14]. On the inertial module is mounted the mannequin with the size and weight of a child (Figure 4).
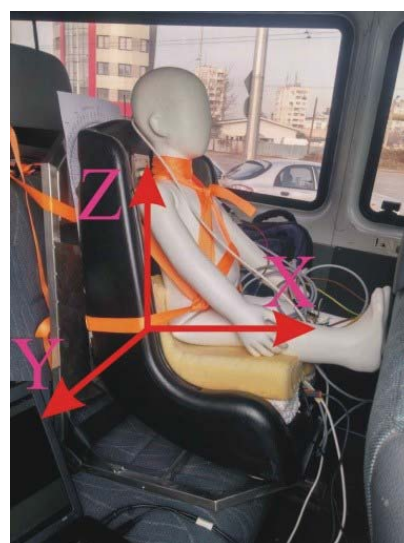

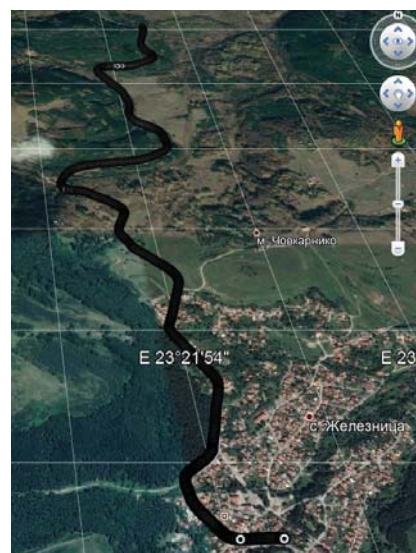Figure 4. The inertial sensor position on the kid car seat

Figure 5. Experimental recorded track

The dynamic test is accomplished on a mountain road with lots of curves. The test road pieces are chosen in such way that the road direction is preliminary from north to south and the road curves are from east to west. The track and the speed are recorded with GPS receiver which is integrated in the inertial system design. The experimental track is shown at Figure 5.

The Euler angles are estimated from the linear accelerations, which are passed through low pass filter with cut-off frequency of 20Hz. Lower cut-off frequency lead to the increased latency of the Kalman filter output towards the acceleration data. Figure 6 represents ϕ angle values when the cut-off frequency is changed from 5 to 20Hz.
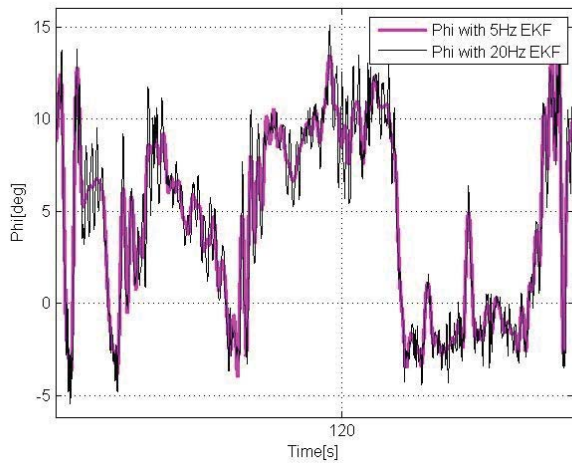
Figure 6. ϕ angle value after low pass filtering with cut-off frequencies from 5 to 20Hz

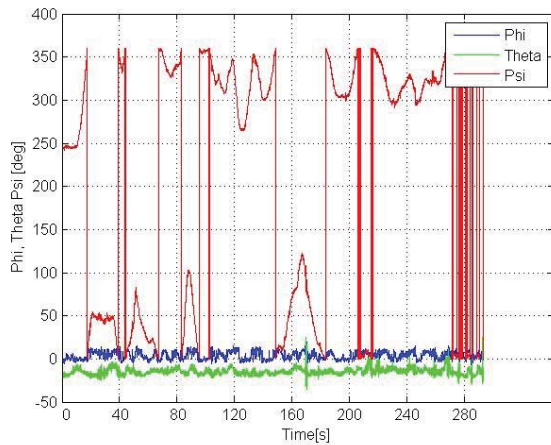The results of the Euler angle estimation are shown at Figure 7.

Figure 7. Estimated Euler angles

The ψ Euler angle values varies from 0 to 360 degrees due to the road curves and the travelling direction, which is constantly changed. We are interested in the ϕ Euler angle because it represents the rotation angle of the kid car seat, which movement is provoked by the lateral accelerations in the curves. The frequency of rotation of the kid car seat is also point of interest because the values represent the travelling comfort [15]. The estimated values of ϕ Euler angle are shown at Figure 8.
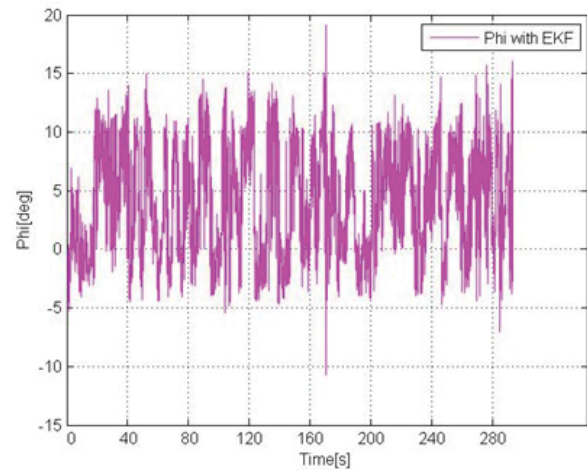

Figure 8. Estimated ϕ Euler angle values (rotation according to X kid car seat axis)

The Euler angles are calculated upon the quaternions model and the results are compared with the EKF ones and can be seen represented at Figure 9.
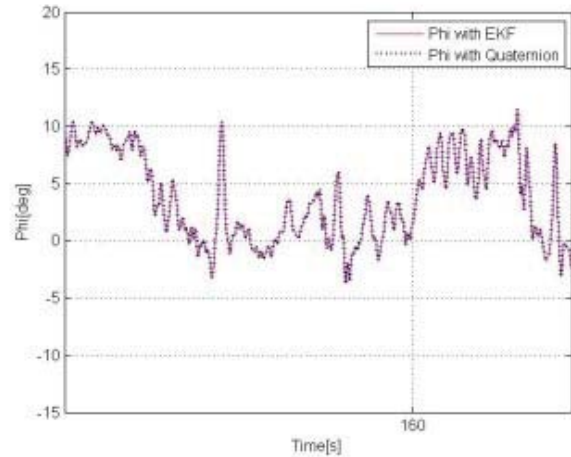

Figure 9. Comparison of the calculated ϕ angle with EKF and quaternions

It shows that there is no apparent difference in the angle values obtained using the two different models.
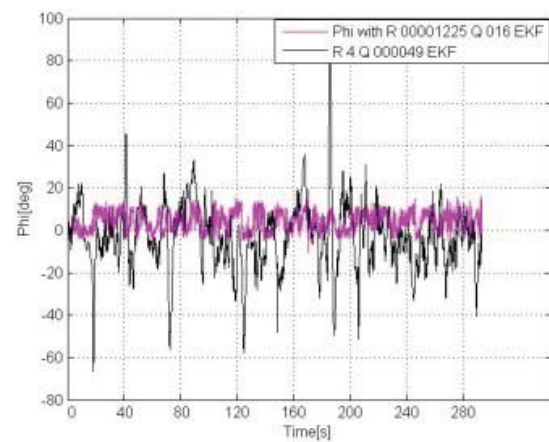

Figure 10. Euler ϕ angle depends from Q and R values

The model parameters are also studied for the Euler angle calculation. The first test (Figure 10, R=0.0001225, Q=0.16) used the noise parameters, which are estimated in our previous paper [16]. When R decreases and Q increases, the contribution of the measurement to the estimate increases. In this case the results match the actual deviation of the kid car seat.

IV. CONCLUSION

The obtained results show that the nonlinear Kalman filter model and the quaternion one represent the similar angle values. The proposed algorithm for the magnetometer calibration and data filtering are adequate. The chosen R and Q values, based on the sensor noise estimation, are included in the model and the results are compared with the real angle values. R and Q values are also studied to the model performance. Better results are obtained when R and Q values correspond to the values of the sensor noise estimation. The cut-off frequency of the low pass filter, which is applied to the accelerometer data, is also studied and it is shown that the lower cut-off frequency lead to the increased latency of the Kalman filter output towards the acceleration data. In the same time, higher cut-off frequency lead to the increased noise levels. Therefore the cut-off frequency of 20Hz is chosen.

REFERENCES

[1] Guochang Xu • Yan Xu, GPS Theory, Algorithms and Applications, Springer, ISBN 978-3-662-50365-2, 2016

[2] Roetenberg Daniel, Inertial and Magnetic Sensing of Human Motion, ISBN-13: 978-90-9020620-2

[3] R. E. Kalman. A New Approach to Linear Filtering and Prediction Problems, ASME Journal of Basic Engineering, series D: 35–45, 1960

[4] Manon Kok, Jeroen D. Hol and Thomas B. Sch¨on (2017), "Using Inertial Sensors for Position and Orientation Estimation", Foundations and Trends in Signal Processing: Vol. 11: No. 1-2, pp 1-153. http://dx.doi.org/10.1561/2000000094

[5] Walter T. Higgins, Jr., A Comparison of Complementary and Kalman Filtering, IEEE Thans. Aerospace and Electronic Systems, Vol. AES-li, no. 3, May 1975

[6] Pedley Mark, Tilt Sensing Using a Three-Axis Accelerometer, Freescale Semiconductor, Document Number: AN3461, Application Note Rev. 6, 03/2013

[7] Lewis Frank L., Shuzhi Sam Ge, Autonomous Mobile Robots Sensing, Control, Decision Making and Applications, Taylor & Francis Group, LLC, 2006, pp 99-149

[8] Jekeli Christopher, Jong-Ki Lee, Inertial/GPS Integrated Geolocation System for Detection and Recovery of Buried Munitions, SERDP Project MR-1565, 2011

[9] Kim Phil, Kalman Filter for Beginners with Matlab Examples, A-JIN Publishing company, 2011, ISBN-13: 978-1463648350

[10] Ozyagcilar Talat, Implementing a Tilt-Compensated eCompass using Accelerometer and Magnetometer Sensors, Freescale Semiconductor, Application Note Document Number: AN4248, Rev. 4.0, 11/2015

[11] Ozyagcilar Talat, Calibrating an eCompass in the Presence of Hard- and Soft-Iron Interference, Freescale Semiconductor, Application Note Document Number: AN4246, Rev. 4.0, 11/2015

[12]http://www.analog.com/static/imported-files/data_sheets/ADIS16400_16405.pdf - datasheet of ADIS16400/ADIS16405 inertial sensor family

[13] Nikolay Pavlov, Evgeni Sokolov, Mihail Peychev, Diana Dacova, Design and test of a tilting seat for improving children's comfort during traveling, Second International Scientific Conference ITEMA 2018 – Conference Proceedings, ISBN 978-86-80194-13-4, pp 305-312

[14] Pavlov N. L., E. E. Sokolov, Tilting Child Safety Seat for Reducing the Lateral Acceleration Acting on Children when Vehicle Cornering, ECCOMAS Thematic Conference on Multibody Dynamics, June 19 - 22, 2017, Prague, Czech Republic, pp 779-783

[15] Pavlov N. L., E. E. Sokolov, M. H. Peychev, D. I. Dacova and L. P. Kunchev, Comfort Improvement and Kinetosis Reduction by the Use of a Pendulum Type Child Travel Seat, International Journal of Mechanical Engineering and Technology (IJMET), Volume 10, Issue 03, March 2019, pp. 277-286. Article ID: IJMET_10_03_028, ISSN Print: 0976-6340 and ISSN Online: 0976-6359

[16] Iontchev E., Simeonov Iv., Miletiev R., Analysis of the Inertial MEMS Sensor Parameters for Navigation Applications, XV International Scientific Conference on Information, Communication and Energy Systems and Technologies, ICEST 2011, Nish, Serbia, June 29 - July 1, 2011, pp 399, ISBN: 978-86-6125-032-3